Original Article

Preparation and characterization of oxybenzone-loaded solid lipid nanoparticles (SLNs) with enhanced safety and sunscreening efficacy: SPF and UVA-PF

Rania A. Sanad[1], Nevine S. Abdel Malak[2],*, Tahany S. El-Bayoomy[1], Alia A. Badawi[2]

[1] *Department of Pharmaceutics, National Organization of Drug Control and Research (NODCAR), Cairo, Egypt;*
[2] *Department of Pharmaceutics, Faculty of Pharmacy Cairo University, Cairo, Egypt.*

ABSTRACT: The objective of the current study was to formulate solid lipid nanoparticles of oxybenzone to enhance its sunscreening efficacy while reducing its side effects. Solid lipid nanoparticles (SLNs) of oxybenzone were prepared by the solvent diffusion method. A complete 2^4 factorial design was used to optimize preparations. The study design involves the investigation of four independent variables, namely lipid type (Glyceryl monostearate, GMS; and Witepsol E85, WE85), lipid concentration (5 and 10%), polyvinyl alcohol (PVA) concentration (1 and 2%), and ethanol/acetone ratios (1:1 and 3:1, v/v), in terms of their effect on the particle size and entrapment efficiency. GMS was found to significantly increase the p.s. and EE%. SLNs prepared using 10% lipid had slower drug release compared to those prepared using 5%. The candidate oxybenzone-loaded SLN formula (SLN2) consisting of 0.5% oxybenzone, 10% GMS, 1% PVA, and ethanol/acetone (1:1, v/v) was then formulated into a gel and compared to the corresponding free oxybenzone nanosuspension and placebo SLN. The formulations were evaluated for skin irritation, *in vitro* sun protection factor, and ultraviolet A protection factors. The incorporation of oxybenzone into solid lipid nanoparticles greatly increased the SPF and UVA protection factor of oxybenzone more than five-fold while providing the advantage of overcoming skin irritancy problems.

Keywords: Solid lipid nanoparticle, oxybenzone, skin irritation, Vitro-Skin®, sun protection factor, UVA protection factor

**Address correspondence to:*
Dr. Nevine Shawky Abdel Malak, Faculty of Pharmacy, Cairo University, Kasr El Ainy Street, 11562 Cairo, Egypt.
e-mail: pharmnova@yahoo.com

1. Introduction

Sunlight is composed of a continuous spectrum of electromagnetic radiation that is divided into three main wavelengths: ultraviolet (UV), visible, and infrared (*1*). UV light is further divided into UVA (320-400 nm), which penetrates the skin and reaches the dermis, causing damage such as immediate and delayed tanning reactions, loss of collagen, diminution in the quantity of blood vessels, and skin photosensitization. UV light is also divided into UVB (290-320 nm), which is the principal cause of sunburn (erythema) and tanning (melanogenesis), and UVC (200-290 nm), which is totally absorbed by the ozone layer (*2*).

The use of sunscreens to protect against harmful UV radiation has become indispensible to daily life due to the worldwide decrease in the ozone layer and the resulting increase in skin cancer incidents (*3*). Sunscreens have been divided into chemical absorbers and physical blockers on the basis of their mechanism of action, namely absorbance and reflection (*4*).

Oxybenzone, a widely used lipophilic, is a broad-spectrum chemical sunscreen agent that effectively absorbs UVB, some UVA, and some UVC light. However, it is the most common cause of photoallergic contact dermatitis (*5*). Systemic absorption of oxybenzone following topical application to the skin has also been reported (*6*). While penetration is desired for drugs, it is not for sunscreens because it leads to loss of activity and undesired side effects (*7*). Therefore, there is an urgent need for the development of safer oxybenzone systems. This can be achieved by formulations that penetrate the skin less or by formulations with a reduced amount of potentially dangerous oxybenzone that maintain the sun protection factor by other means, *e.g.* carriers with sun-blocking characteristics (*3*).

Solid lipid nanoparticles have served as carriers for various pharmaceutical and cosmetic actives. These lipid nanoparticles have been found to act as physical sunscreens on their own, *i.e.* they have the ability to scatter/reflect incoming UV radiation. Incorporation of chemical sunscreens into the solid lipid matrix of the solid

lipid nanoparticle (SLN) prevents penetration of the skin and resulting side-effects (*4*).

The solvent diffusion method is a technique for preparing SLNs. This technique is characterized by using pharmaceutically acceptable organic solvents, easy handling, and a fast production process (*8*).

The UV protection properties of the nanoparticles can be described in terms of the sun protection factor (SPF) like in the case of any other sunscreen product. However, the SPF mainly represents the protection against UVB. For this reason, newly developed sunscreens have to provide a description of the protection they provide against not only UVB radiation but also UVA radiation (*9*).

Vitro-Skin®, a registered trademark of IMS Inc. (Portland, ME, USA), is an advanced testing substrate used for *in vitro* measurement of SPF. It contains both optimized protein and lipid components and is designed to have topography, pH, critical surface tension, and ionic strength similar to human skin (*10*). This substrate provides the most consistent correlation with published *in vivo* SPF measurements (*11*).

The present study attempted to prepare and evaluate oxybenzone-loaded SLNs. A candidate formula with optimum physicochemical characterization was then selected. This formula was then formulated into a gel. A skin irritation test was performed and the *in vitro* SPF and UVA protection factor of free oxybenzone and the selected formula before and after its formulation into a gel were measured using Vitro-Skin®. Previously published research has not used Vitro-Skin® to determine the SPF and UVAPF of sunscreen in SLNs.

2. Materials and Methods

2.1. *Materials*

Oxybenzone was obtained from International Specialty Products, USA. Glyceryl monostearate (GMS), which is a mixture of 40-50% mono-, 30-45% di-, and 5-15% triglycerides esters of stearic acid (C_{21}) and palmitic acid (C_{19}) with a melting point of 55-66°C, was obtained from Carl Roth GmbH, Karlsruhe, Germany. Witepsol E85 (WE85), which is a mixture of 5% mono-, 29% di-, and 66% triglycerides esters of fatty acids (C_8-C_{18}) and with a melting point 42-44°C, was obtained from Dynamit-Nobel Chemicals, Germany. Polyvinyl alcohol (PVA) of average molecular weight 146,000-186,000 was obtained from Celanese, Dallas, TX, USA. Ethanol 95% and acetone were obtained from Honeywell Riedel-de Haen, Seelze, Germany. Carbopol 934 was obtained from Goodrich Chemical Co., Avon Lake, OH, USA. Vitro-Skin® was obtained from IMS Inc. (Portland, ME, USA). Transpore™ Surgical Tape was obtained from 3M Australia Pty Ltd., Pymble, NSW, Australia. A hydrophobic filter assembly, a membrane filter with 0.2-μm diameter pores, was obtained from Versapor, German Sciences, Germany. All other chemicals and solvents were of analytical grade.

2.2. *Design of the experiments*

A complete 2^4 factorial design was used to optimize preparations of oxybenzone SLNs. The study design involved the investigation of four independent variables, namely lipid type, lipid concentration, PVA concentration, and organic solvent ratio, and their effect on the particle size and entrapment efficiency of oxybenzone SLNs. Table 1 summarizes independent variables along with their levels. The experimental results were analyzed using StatView version 4.57 software (Abacus Concept, Piscataway, NJ, USA).

2.3. *Preparation of oxybenzone SLNs*

SLNs loaded with 5% oxybenzone were prepared by the solvent diffusion method in an aqueous system (*12*) with slight modification. The amount of the drug to be added (in grams) was calculated as a percentage of the lipid matrix as follows: 100 g of a 10% SLNs dispersion loaded with 5% drug containing 10 g solid consisting of 9.5 g lipid and 0.5 g drug (*13*). The lipid-oxybenzone mixture was completely dissolved in a 12-mL mixture of ethanol and acetone (1:1 or 3:1, v/v) in a water bath at 50°C. The resultant lipid solution was poured into 240 mL of an aqueous phase containing PVA (1 or 2%, w/v) under mechanical agitation using a mechanical stirrer (Falc Instruments, Treviglio, Italy) at 400 rpm in a water bath at 70°C for 5 min. The obtained dispersion was allowed to cool to room temperature while stirring with a magnetic stirrer to get rid of the organic solvents, and then oxybenzone-loaded SLNs were finally obtained. The placebo SLN dispersions were prepared exactly in the same manner without adding the drug (*14*). An overview of the composition of the SLNs is shown in Table 2.

2.4. *Characterization of oxybenzone SLNs*

2.4.1. *Transmission electron microscopy (TEM)*

The morphology of the oxybenzone SLNs (selected samples SLN2 and SLN10) was examined with a transmission electron microscope (JEM-100S, Jeol Ltd.,

Table 1. Planned 2^4 factorial design for the optimization of the prepared oxybenzone SLN dispersions

Independent variables	Levels	
	+1	−1
Type of lipid	GMS	WE85
Concentration of lipid (%, w/w)[a]	5	10
Concentration of PVA (%, w/w)[a]	1	2
Organic solvent ratio (ethanol/acetone, v/v)[b]	1:1	3:1

[a] Percentage of the final SLN dispersion; [b] Ratio with respect to the total organic solvent mixture.

Table 2. Composition of the prepared oxybenzone SLN dispersions

Formulation code	Lipid Type		PVA (%, w/w)[a]	Ethanol (mL)[b]	Acetone (mL)[b]	Oxybenzone (%, w/w)[a]
	GMS (%, w/w)	WE85 (%, w/w)				
SLN1	5	0	1	6	6	0.25
SLN2	10	0	1	6	6	0.5
SLN3	5	0	1	9	3	0.25
SLN4	10	0	1	9	3	0.5
SLN5	5	0	2	6	6	0.25
SLN6	10	0	2	6	6	0.5
SLN7	5	0	2	9	3	0.25
SLN8	0	0	2	9	3	0.5
SLN9	0	5	1	6	6	0.25
SLN10	0	10	1	6	6	0.5
SLN11	0	5	1	9	3	0.25
SLN12	0	10	1	9	3	0.5
SLN13	0	5	2	6	6	0.25
SLN14	0	10	2	6	6	0.5
SLN15	0	5	2	9	3	0.25
SLN16	0	10	2	9	3	0.5

[a] Percentage in the final SLN dispersion; [b] Volume in the final SLN dispersion.

Tokyo, Japan). Samples were prepared by a negative staining technique. The SLNs were dispersed directly into doubly distilled water. Then, a copper grid coated with collodion film was placed in the solution several times. After staining with 2% (w/v) phosphotungstic acid solution and drying at room temperature, the sample was ready for TEM investigation at 70 kV (*15*).

2.4.2. *Particle size analysis*

Particle size and polydispersity index (PI) were determined using a laser scattering particle size distribution analyzer (detection limit 0.2-2,000 μm; LA-920, Horiba, Kyoto, Japan). One day after production, SLN dispersions were diluted with filtered doubly distilled water and subsequently analyzed. Three analyses were performed for each sample and the average values were used. The obtained data were evaluated using the volume distribution (d10%, d50%, d90%). This meant that if the diameter 90% (d90%) was registered as 1 μm then 90% of particles would have a diameter of 1 μm or less (*16*).

2.4.3. *Determination of percent oxybenzone entrapment efficiency (% EE)*

The entrapment efficiencies of prepared systems were determined by measuring the concentration of free drug in the dispersion medium. The drug-loaded SLN dispersion was uniformly mixed by gentle shaking; 1.0 mL of this dispersion was diluted with 9.0 mL methanol, centrifuged with a high-speed refrigerated centrifuge (Sigma 3K30, DJB Labcare, Buckinghamshire, UK) for 45 min at 16,000 rpm and then filtered using a Millipore membrane (0.2 μm). The filtrate was collected and appropriately diluted with methanol and measured spectrophotometrically (Model UV-2450, Shimadzu,

Kyoto, Japan) at a λ_{max} of 286 nm. The percent entrapment efficiency % EE was calculated using the following equation (*14*):

$$\text{Entrapment Efficiency (\% EE)} = \frac{\text{Wa} - \text{Ws}}{\text{Wa}} \times 100$$
--- Eq. 1

where Wa and Ws were the weight of drug added in system and the analyzed weight of drug in supernatant, respectively.

2.4.4. *In vitro release studies of oxybenzone from SLNs: Franz diffusion cells*

In vitro release studies of oxybenzone were done using static Franz glass diffusion cells (*17*). These cells consist of donor and receptor chambers separated by a cellulose membrane (MEMBRA-CEL dialysis tubing with molecular weight cutoff of 3,500-7,000 Da obtained from Serva Electrophoresis GmbH, Heidelberg, Germany); the area of diffusion was 1.7 cm^2. The dialysis membrane was hydrated in receptor medium, which consisted of a methanolic buffer solution (phosphate-buffered saline, pH7.4/methanol, 3:2, v/v), for 12 h before mounting into a Franz diffusion cell. An oxybenzone SLN dispersion (2 mg/cm^2) was placed in the donor chamber and the receptor chamber was filled with 7.5 mL receptor medium and stirred continuously at 100 rpm at 37°C in order to ensure a surface skin temperature of 32°C on the surface of the membrane (*17*). After 1, 2, 3, 4, 5, 6, 7, and 8 h, samples were withdrawn from the receptor chamber through a side-arm tube. After each withdrawal of sample, an equal volume of receptor medium was added to the receptor chamber to maintain a constant volume throughout the study. Samples were analyzed for oxybenzone concentration using ultraviolet spectrophotometry at 289.4 nm. Measurements were carried out in triplicate.

Table 3. Composition of the selected dispersions and corresponding gel formulations

Formulation	Composition
pSLN2	10% GMS, ethanol/acetone (1:1, v/v) in 1% PVA aqueous solution
SLN2	0.5% oxybenzone (with respect to total formulation), 10% GMS, ethanol/acetone (1:1, v/v) in 1% PVA aqueous solution
0.5% Oxy.	0.5% oxybenzone (with respect to total formulation), ethanol/acetone (1:1, v/v) in 1% PVA aqueous solution
pSLN2G	1% carbopol 934 incorporated in pSLN2 dispersion
SLN2G	1% carbopol 934 incorporated in SLN2 dispersion
0.5% Oxy.G	1% carbopol 934 incorporated in 0.5% oxybenzone dispersion

2.5. *Formulation of an SLN-based hydrogel*

Based on the previously described characterization, SLN2 with optimal physicochemical properties was selected. The selected SLN dispersion was formulated into a hydrogel by adding 1% (w/w) Carbopol 934 under magnetic stirring at 800 rpm. Stirring was continued till Carbopol was dispersed. The dispersions were neutralized using triethanolamine solution (*18*). Hydrogel formulations containing 0.5% oxybenzone suspension and placebo SLN2 were prepared for comparison. The composition of gel formulations is shown in Table 3.

2.6. *Characterization of the prepared gels*

2.6.1. *Rheological studies*

The viscosity and rheological behavior of the gel formulations were determined using a Cone and Plate viscometer (model HADV-II; Brookfield Engineering Laboratories, Middleboro, MA, USA). All measurements were carried out at a temperature of 25 ± 1°C using a spindle CP52. The rheological parameters of different gels were studied (*19*).

2.6.2. *Skin irritation test*

The study protocol and informed consent form were approved by an institutional review board (IRB00007140), and this study was conducted in accordance with the Declaration of Helsinki (*20*) and the Guidance for Good Clinical Practice of the International Conference on Harmonization (ICH) of Technical Requirements for Registration of Pharmaceutics for Human Use (*21*).

Ten healthy subjects (ages 23-40 years) participated in this study. The participants were briefed on the study procedures, and written informed consent was obtained prior to procedures. Each formulation mentioned in Table 3 was applied once, at a dose of 0.3 g, to a surface area of 5 cm^2 on the forearms. The test specimen was then washed off with tap water after 6 h and skin was observed for any visible changes such as erythema (redness). The mean erythemal scores were recorded (ranging from 0 to 4) in accordance with the Draize scale (*22*) as shown in Table 4.

Table 4. Draize grading scale (erythema formation)

Skin response	Score
No erythema	0
Slight erythema (barely perceptible-light pink)	1
Moderate erythema (dark pink)	2
Moderate to severe erythema (light red)	3
Severe erythema (extreme redness)	4

2.6.3. *In vitro UV-blocking ability*

Transpore™ assay (*7*) is an *in vitro* method of investigating the UV-blocking ability of the investigated dispersions mentioned in Table 3. A concentration of 2 mg/cm^2 of the formulation was spread evenly on top of the Transpore™ tape mounted on a quartz cuvette. After a drying period of 15 min, the samples were scanned spectrophotometrically from 250 to 400 nm and the absorption was measured.

2.6.4. *In vitro SPF and erythemal UVA protection factor (EUVA-PF) measurement*

Determination of the SPF of the formulations was done in accordance with the method described by Diffey and Robson (*24)*. Vitro-Skin® was used for sample application. It was hydrated by placing it on the shelf of a closed, controlled-humidity chamber (containing 85% water/15% glycerin in its bottom) for 16-24 h prior to use (*23*) and then mounted on a quartz cuvette. The intensity of radiation transmitted through the substrate was determined automatically by recording the photocurrent in 5-nm increments from 290 to 400 nm. An appropriate weight (2 mg/cm^2) of each formulation mentioned in Table 3 was applied to the substrate surface by applying spots to several sites throughout the application area (4.5 cm^2). After a drying period of 15 min, transmission measurements were done. These experiments were performed in triplicate.

The *in vitro* SPF was calculated according to the following equation (*24*):

$$SPF = \sum_{290}^{400} E_\lambda B_\lambda \Big/ \sum_{290}^{400} (E_\lambda B_\lambda \sqrt{MPF_\lambda}) \qquad \text{--- Eq. 2}$$

where E_λ was the spectral irradiance of terrestrial sunlight under defined conditions, B_λ was erythemal effectiveness, and MPF_λ was the monochromatic protection factor at each wavelength increment measured as the ratio of

the detector signal intensity without sunscreen applied to the substrate to that with sunscreen applied to the substrate. Given the UVA wavelength range (320-400 nm) and using the terms in the SPF equation, the *in vitro* erythemal UVA protection factor was calculated according to the following equation (*9*):

$$\text{Erythemal UV-A protection factor} =$$

$$\sum_{320}^{400} E_\lambda B_\lambda / \sum_{320}^{400} (E_\lambda B_\lambda \sqrt{MPF_\lambda}) \qquad \text{--- Eq. 3}$$

3. Results and Discussion

3.1. *Characterization of oxybenzone solid lipid nanoparticles*

3.1.1. *TEM*

Figure 1 shows transmission electron micrographs of oxybenzone SLNs prepared with GMS and WE85 as lipid bases using the solvent diffusion technique. Both micrographs showed that the particles had nanometer-
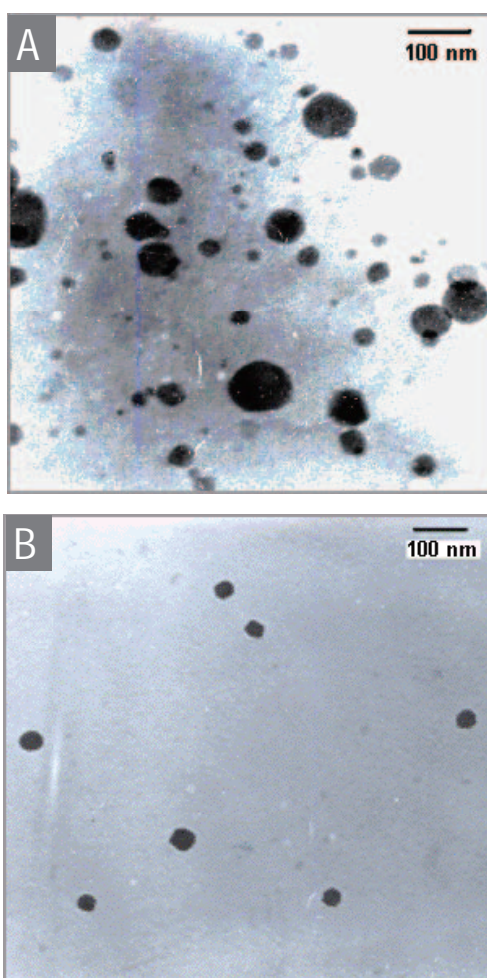
Figure 1. Transmission electron micrographs of oxybenzone-loaded SLNs using GMS (A) and WE85 (B) prepared by the solvent diffusion method in an aqueous system. Scale bar, 100 nm.

sized spherical shapes ranging from 20 to 100 nm for GMS SLNs and from 30 to 50 nm for WE85 SLNs; no rectangular oxybenzone crystals were visible. This could be due to the solvent diffusion procedure during the solvent diffusion to dispersion medium; the lipid matrix might form nanoparticles with a spherical shape to minimize surface energy (*25*). In addition, the use of GMS and WE85, which are considered to be chemically heterogeneous lipids that are mixtures of mono-, di-, and triglycerides in different portions, favored the formation of ideally spherical lipid nanoparticles (*26*).

3.1.2. *Particle size analysis*

In order to obtain more precise information on the size distribution, laser scattering was used (*27*). The mean particle size, volume size distribution (d10%, d50%, and d90%), and span (which is the measure of polydispersity index) of different SLNs are depicted in Table 5.

The results revealed that all of the prepared SLNs had a considerable small particle size with d90% less than 1 μm. The mean particle size of SLNs ranged from 0.209 ± 0.020 to 0.810 ± 0.032 μm. The sizes of the SLNs determined by laser scattering did not agree with TEM results. This might be because detection of the size of SLNs using laser scattering was carried out in an aqueous state. In such instances, lipid nanoparticles were highly hydrated and the diameters were 'hydrated diameters' that tended to be larger than their genuine diameters. In TEM sample preparation, all of the free water and even some of hydrated water was stained. This implies that the sizes of SLNs determined by TEM might be considerably smaller than their real diameters (*28*). The span values (Table 5), a characteristic parameter for the extent of particle size distribution, ranged from 0.347 to 0.687 for GMS SLNs and from 0.529 to 0.611 for WE85 SLNs. According to Muller and Schumann (*29*), these values contributed to a relatively broad size distribution. That said, a polydispersed particle dispersion is suitable for topical application (*30*).

Statistical analysis was done to evaluate the effect of the lipid type, the lipid concentration, the PVA concentration, and the organic solvent ratio on the particle size. GMS was found to significantly increase the particle size compared to WE85 ($p < 0.0001$). This could be due to GMS possessing a higher melting point (54-66°C) (*31*) than WE85 (42-44°C) (*31*) or to the fact that the average particle size of SLNs increases with higher melting lipids, indicating an effect of the higher viscosity of the dispersed phase (*32*). Additionally, lipids of shorter chain length have been found to yield SLNs of smaller particle size in comparison to those produced by lipids of longer chains (*33*). Therefore, WE85, which consists of glycerides with shorter hydrocarbon chains (C_8-C_{18}) compared to GMS (C_{19} and C_{21}) (*31*), produced smaller particles.

Table 5. Particle size distribution, mean particle size, polydispersity index, entrapment efficiency, and zeta potential values of different solid lipid nanoparticles dispersions

Formulation code[a]	Mean volume distribution (μm)			Mean particle size (μm, mean ± S.D.)	PI[b]	EE% (mean ± S.D.)	Zeta potential (mean ± S.D.)
	d10%	d50%	d90%				
SLN1	0.090	0.206	0.389	0.297 ± 0.011	0.341	44.8 ± 1.9	−12.3 ± 0.5
SLN2	0.200	0.389	0.704	0.590 ± 0.029	0.528	74.2 ± 2.5	−47.0 ± 0.8
SLN3	0.159	0.259	0.616	0.347 ± 0.02	0.531	43.2 ± 1.5	−14.9 ± 0.6
SLN4	0.281	0.540	0.961	0.420 ± 0.023	0.483	72.8 ± 1.1	−21.5 ± 1.2
SLN5	0.215	0.389	0.751	0.443 ± 0.018	0.513	48.0 ± 2.3	−12.8 ± 0.7
SLN6	0.220	0.390	0.833	0.474 ± 0.03	0.510	60.6 ± 3.5	−12.6 ± 0.3
SLN7	0.178	0.296	0.676	0.375 ± 0.026	0.557	38.4 ± 2.1	−10.6 ± 1.0
SLN8	0.564	0.800	0.968	0.810 ± 0.032	0.687	54.6 ± 1.6	−17.8 ± 0.5
SLN9	0.136	0.197	0.295	0.209 ± 0.02	0.581	30.0 ± 0.8	−19.9 ± 0.8
SLN10	0.166	0.276	0.759	0.383 ± 0.024	0.529	41.1 ± 1.3	−8.8 ± 0.6
SLN11	0.171	0.238	0.361	0.258 ± 0.019	0.611	27.7 ± 1.8	−20.9 ± 0.9
SLN12	0.159	0.259	0.599	0.335 ± 0.01	0.543	38.4 ± 2.4	−26.5 ± 2.0
SLN13	0.178	0.283	0.587	0.349 ± 0.022	0.558	24.6 ± 0.9	−14.7 ± 0.9
SLN14	0.182	0.265	0.481	0.322 ± 0.015	0.585	38.5 ± 3.1	−47.6 ± 1.3
SLN15	0.142	0.201	0.303	0.230 ± 0.017	0.606	10.9 ± 0.8	−27.8 ± 2.0
SLN16	0.190	0.296	0.948	0.494 ± 0.01	0.572	32.5 ± 1.4	−13.1 ± 2.5

[a] The composition of these formulations is shown in Table 2; [b] Polydispersity index.

Among the lipid concentrations used, 10% resulted in a significantly larger particle size than did 5% ($p < 0.0001$). When the concentration of lipid (GMS or WE85) was increased, the viscosity of the lipid-organic solvent diffusion phase also increased. This reduced the diffusion rates of the solute molecules, which are a critical parameter for the formation of SLNs prepared by the solvent diffusion method. In addition, the collision and aggregation of nanoparticles, which were facilitated by a high lipid concentration, led to the formation of larger particles (*8,34*).

Among the PVA concentrations used, 1% PVA was found to result in a significantly smaller particle size than did 2% ($p < 0.0001$). This might be due to the fact that the increase in PVA concentration from 1 to 2% increased the viscosity of the external aqueous phase (*35*). This resulted in a decrease in the net shear stress, reducing the diffusion speed and therefore increasing particle size (*36*). In addition, higher concentrations of the stabilizer (2% PVA) would not play any further role with regard to particle size once the optimum packing of the stabilizer (PVA) and the minimum droplet size was reached (*37*). Further addition of PVA caused an increase in nanoparticle size due to the accumulation of excess molecules at the particle surface; loops and tails were formed, eventually leading to bridging between the primary nanoparticles (*38*).

Concerning the effect of different ratios of organic solvents, ethanol:acetone at a ratio of 1:1 (v/v) was found to significantly decrease the particle size compared to 3:1 (v/v) ($p < 0.0001$), which meant that increasing the ethanol volume led to an increase in the particle size while increasing the acetone volume caused a decrease in the particle size of the prepared SLNs. This may be due to the lower boiling point of acetone (56.53°C) (*31*) compared to that of ethanol

(78.4°C) (*31*), so an organic solvent mixture (ethanol/acetone) at a ratio of 1:1 (v/v) would evaporate more rapidly than one at a ratio of 3:1 (v/v) (*39*). The higher organic solvent evaporation rate led to a higher solvent front kinetic energy, which accordingly increased the rate of diffusion of the solvent from the inner to the outer phase (the critical parameter determining the particle size) and resulted in smaller particles (*40*).

3.1.3. *Zeta potential ζ*

The zeta potential ζ values of the prepared SLNs are shown in Table 5. The values ranged from −8.8 mV to −47 mV. Zeta potential values of all formulations in this study were above |8-9| mV, which is a prerequisite for the stability of SLNs prepared using a steric stabilizer (PVA) (*41*). All SLNs were found to be negatively charged. This negative charge was likely caused by the slightly ionized fatty acids from the glycerides used (GMS and WE85) (*42*). Zeta potentials above |30 mV| were required for full electrostatic stabilization. However, many experiments demonstrated that electrostatic repulsion had the greatest impact on the stability of nanoparticles; the use of steric stabilizer also favored the formation of a stable nanoparticle dispersion (*26*).

3.1.4. *Entrapment efficiency*

The entrapment efficiency of oxybenzone within the different prepared SLNs is shown in Table 5. The entrapment efficiencies were found to range between 20.9 ± 0.8% and 74.3 ± 2.5%.

Concerning the effect of the lipid type, GMS was found to significantly increase the entrapment efficiency compared to WE85 ($p < 0.0001$). This could be due to an increase in the ratio of monoglycerides to more than

30% (GMS consists of 40-50% monoglycerides while WE85 consists of 5% monoglycerides), which might offer more room to accommodate the drug in the lipid matrix (*43*). In addition, the entrapment efficiency of the prepared SLNs increased as a result of the increased lipophilicity of the lipids used (*44*). GMS (C_{21}) is more lipophilic than WE85 (C_8-C_{18}) (*31*) since an increase in the alkyl chain length led to an increase in the lipophilicity of the molecule (*45*). As a result, GMS had greater accommodation for the lipophilic drug (oxybenzone) than did WE85. In addition, particles of larger sizes have been reported to possess higher entrapment efficiency (*46*). Therefore, the higher entrapment efficiency of GMS SLNs contributed to their larger particle size compared to WE85 SLNs.

A lipid concentration of 10% significantly increased the entrapment efficiency compared to a concentration of 5% (*p* < 0.0001). This could be due to the increase in the lipid concentration (10%), which led to increased lipophilicity that significantly increased the entrapment efficiency of oxybenzone. This agrees with the findings of Shah *et al.* (*18*), who observed that the entrapment efficiency of a drug increased in accordance with an increase in the amount of lipids.

Increasing the PVA concentration from 1 to 2% was found to significantly decrease the entrapment efficiency of oxybenzone within the prepared SLNs (*p* < 0.0001). One possible interpretation is that 1% PVA concentration provided sufficient covering of the lipid core so as to minimize possible leaching of the drug (*15*), while with an increased PVA concentration (2%) more molecules of the drug partitioned out rapidly into the aqueous phase during the emulsification procedure due to the solubilizing and emulsifying effect of PVA (*47*). As a result, the entrapment efficiency decreased (*38*). This agrees with the findings of Paliwal *et al.* (*15*), who observed that the entrapment efficiency decreased when the amount of the emulsifier was increased.

With regard to ratios of organic solvents, a 1:1 (v/v) ethanol/acetone ratio provided significantly higher entrapment efficiency than did one of 3:1 (v/v). This increase in entrapment efficiency could be due to the increased ratio of ethanol, which might act as a co-emulsifier (*48*). As the amount of co-emulsifier increased with a constant amount of lipid, the surface of the SLNs formed was too small to adsorb all of the co-surfactant molecules. This might result in the formation of micellar solutions of the drug (oxybenzone). Hence the solubility of the drug in the water phase would increase. Therefore, the drug could partition from the SLNs into the formed micelles in the water phase, thereby reducing the final entrapment efficiency (*38*).

3.1.5. *In vitro release study: Franz diffusion cells*

The release of oxybenzone from SLNs was investigated for 8 h. The composition of the receptor medium was chosen because of the insufficient solubility of oxybenzone in aqueous media. Oxybenzone was readily soluble in the chosen receptor medium. Since the receptor medium was not intended to mimic skin conditions, it was adequate for the present *in vitro* investigations. Figure 2 shows the release of oxybenzone from the prepared SLNs.
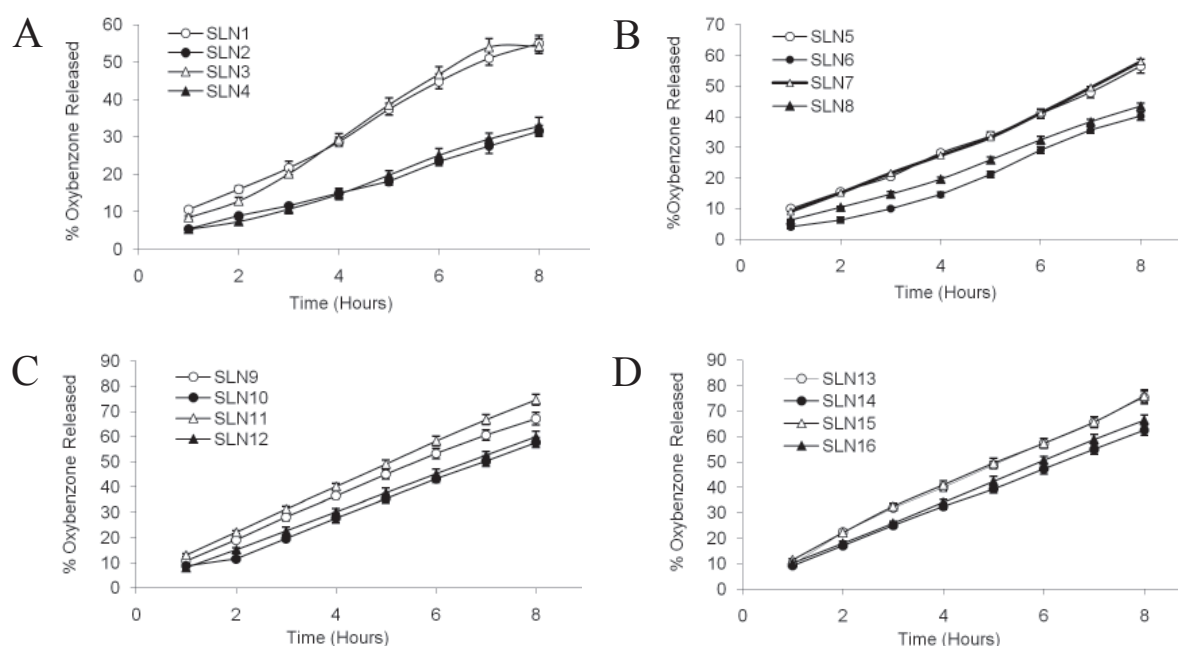
Figure 2. *In vitro* release profile of oxybenzone from different oxybenzone-loaded SLNs in phosphate-buffered saline, pH 7.4/methanol (3:2, v/v). (A) open circle, SLN1; closed circle, SLN2; open triangle, SLN3; closed triangle, SLN4. **(B)** open circle, SLN5; closed circle, SLN6; open triangle, SLN7; closed triangle, SLN8. **(C)** open circle, SLN9; closed circle, SLN10; open triangle, SLN11; closed triangle, SLN12. **(D)** open circle, SLN13; closed circle, SLN14; open triangle, SLN15; closed triangle, SLN16. Data are shown as mean ± S.D., *n* = 3.

GMS SLNs were found to have slower release than did WE85 SLNs. Slow release of the drug from SLNs suggests homogeneous entrapment of the drug throughout the system (*15*). Consequently, GMS SLNs with higher entrapment efficiency than WE85 SLNs had slower release profiles. Other factors contributing to a fast release might be the large surface area and the high diffusion coefficient (small molecular size) (*49*). Therefore, WE85 SLNs with a smaller particle size and consequently higher surface area than GMS SLNs had more rapid release.

Among the lipid concentrations used, oxybenzone was released more easily from SLNs containing a lower lipid content (5%) than a high one (10%). Similar results were obtained by Souto *et al*. (*50*), who attributed this to the possible formation of a drug-enriched shell as SLNs might develop when using a low lipid concentration. At higher lipid concentration, a drug-enriched core was formed and lower release was observed.

In terms of PVA concentration, 2% PVA was found to result in faster release than 1% (w/w) PVA. This might be due to the diffusion of surfactant (PVA) into the receiver side, altering the barrier properties of the aqueous boundary layer and the permeability of the membrane and subsequently resulted in a high release velocity of drug in the SLN dispersion (*51*). Moreover, the existence of a large amount of surfactant increased the solubility of the drug in water, resulting in the re-partitioning of drug into the water phase. This allowed spots of the drug domain to be formed on the surface of the SLNs, resulting in faster release (*52*).

Based on previous characterizations, the SLN2 dispersion prepared using 10% GMS, 1% PVA, and a 1:1 (v/v) ethanol/acetone ratio had the highest EE%, the slowest drug release, the highest zeta potential, and a sufficiently small particle size, so it was chosen for formulation into a gel. The rheological properties, irritancy, UV blocking ability, SPF, and UVA-PF were studied and compared with that of placebo SLN2 and an oxybenzone suspension containing a concentration like that of SLN2 (0.5% with respect to the total formulation).

3.2. Characterization of the prepared gels

3.2.1. Rheological studies

As previously noted, conventional SLN aqueous dispersions contain about 10-20% (w/w) of lipid matrix and 80-90% (w/w) of water. As a result, liquid solid lipid dispersions possess a low viscosity. Therefore, liquid solid lipid dispersions usually have to be incorporated in convenient topical dosage forms like hydrogels to obtain a topical application form with the desired semisolid consistency (*53*).

Carbopol hydrogels have proven suitable for nanoparticle incorporation (*54*). Thus, this study used Carbopol 934 because of its thermal stability, mucoadhesive properties, and optimal rheological properties in order to prepare semi-solid formulations based on SLNs (*55*).

The rheological properties of a semisolid drug carrier are very important physical parameters for a topical application of that drug (*56*). Figure 3 shows the rheograms of the prepared gel formulations. The results revealed that gel formulations containing SLN2, either as a placebo or oxybenzone-loaded SLNs, exhibited pseudoplastic flow characteristics with thixotropy. Needless to say, thixotropy is a desirable feature for semisolid drug carriers for use in a topical application (*57*). As shown in Figures 3A and B, SLN2 gel formulations, either as a placebo or oxybenzone-loaded SLNs, had greater thixotropy (hysteresis area). This could be due to the negatively charged SLNs, which may affect the restoration of hydrogen bonding in the gel. Therefore, restructuring of the three-dimensional network structure took longer and consequently increased the thixotropy of SLN-enriched gels (*56*).
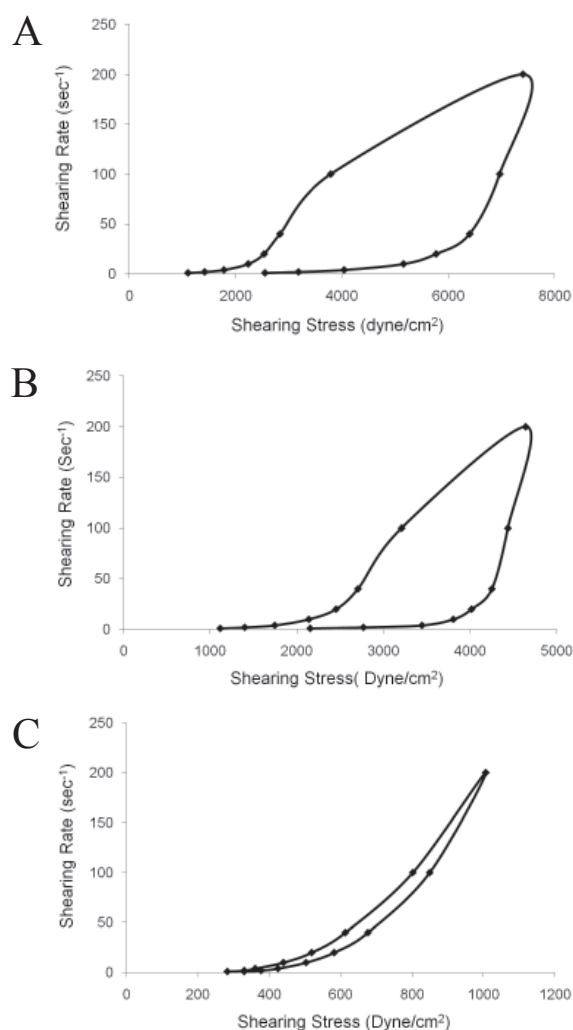
Figure 3. Rheograms of placebo SLNG (A), SLN2G (B), and 0.5% free oxybenzone gels (C).

Table 6. Results from a skin irritation test of the selected dispersions and corresponding gel formulations

Formulation[a]	Reaction in volunteers[b]									
	Subject 1	Subject 2	Subject 3	Subject 4	Subject 5	Subject 6	Subject 7	Subject 8	Subject 9	Subject 10
pSLN2	0	0	0	0	0	0	0	0	0	0
SLN2	0	0	0	1	0	1	0	0	0	0
0.5% Oxy.	2	2	2	2	2	3	2	1	2	2
pSLN2G	0	0	0	0	0	0	0	0	0	0
SLN2G	0	0	0	1	0	1	0	0	0	0
0.5% Oxy.G	2	2	2	3	2	3	2	2	2	2

[a] The composition of these formulations is shown in Table 3; [b] The scoring system is described in Table 4.

3.2.2. *Skin irritation test*

Results of the skin irritation test are shown in Table 6. No irritation or erythema was observed for placebo SLN2 either in dispersion or gel form, and only very slight erythema (score = 1) was observed in two volunteers with an oxybenzone-loaded SLN2 dispersion or gel. Conversely, a 0.5% oxybenzone suspension and gel resulted in well defined erythema in seven volunteers (score = 2) and moderate to severe erythema (score = 3) in two volunteers. This could be due to the role of oxybenzone-loaded SLN2 in protecting the skin from direct contact with the drug (oxybenzone), which was encapsulated in the lipid matrix. Such encapsulation allows for gradual drug delivery and paves the way to reducing drug-induced skin irritation (*58*). This agrees with the findings of Küchlera *et al*. (*59*), who observed that drug-loaded SLNs were significantly less irritating to the skin compared to the effects of marketed products containing the drug in free form.

3.2.3. *In vitro UV-blocking ability*

The wavelength scans of the placebo SLN2, oxybenzone-loaded SLN2, and 0.5% oxybenzone dispersions are shown in Figure 4. The absorbance caused by placebo SLN2 was found to be higher than the absorption caused by the 0.5% oxybenzone suspension. This could be due to the particulate character of SLNs since they act as physical sunscreens on their own (*60*). This agrees with the findings of Wissing and Muller (*4*), who observed that placebo SLNs were more effective as a sunscreen than reference emulsions containing tocopherol acetate.

Oxybenzone-loaded SLN2 was also found to have a typical absorption pattern of oxybenzone with two peaks at about 340 and 290 nm, indicating that oxybenzone-loaded SLN2 still had absorption in the UVB range (290-320 nm) and the UVA range (320-400 nm). That said, this absorption was about three times higher than the absorbance caused by the 0.5% oxybenzone suspension. This could be due to the fact that the incorporation of chemical sunscreens (oxybenzone) in SLNs led to synergistic UV-blocking behavior (*60*). Similarly, Song *et al*. (*61*) observed that 3,4,5-trimetho xybenzoylchitin (sunscreen) had higher UV absorption
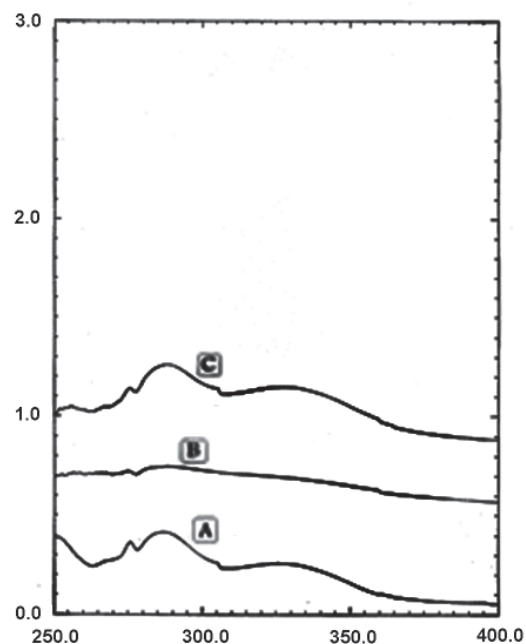
Figure 4. Wavelength scans of 0.5% oxybenzone nanosuspension (0.5% Oxy.) (A), placebo SLN dispersion (PSLN) (B), and oxybenzone-loaded SLN dispersion (SLN2) (C) obtained by the Transpore™ tape assay.

when it was incorporated in SLNs as a vehicle because SLNs provide stronger reflectance of UV radiation.

3.2.4. *In vitro SPF and EUVA-PF measurement*

The SPF values of the investigated formulations are illustrated graphically in Figure 5. The placebo SLN2 dispersion had a higher SPF value (4.90 ± 0.42) than did the suspension containing 0.5% oxybenzone without lipids (1.80 ± 0.12). When SLN2 was loaded with 0.5% oxybenzone, the resulting SPF values increased by about 6-fold compared to those of the 0.5% oxybenzone suspension (11.13 ± 0.70).

The EUVA-PF is a parameter analog to the SPF and it represents a number derived from the ratio for the duration of exposure to a UV spectrum between 320 nm and 400 nm to produce erythema on human skin in the presence or absence of a sunscreen product. The higher the value, the more UVA protection a sunscreen offers (*9*). Figure 6 shows that 0.5% oxybenzone alone had
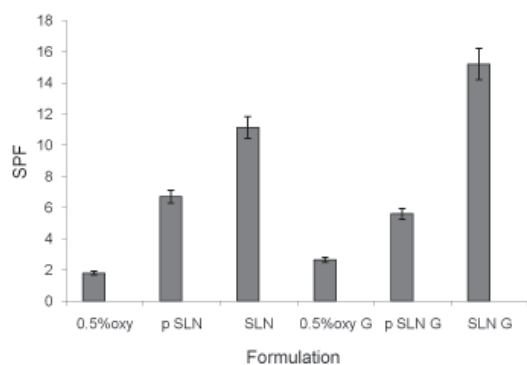
Figure 5. SPF values of different SLNs formulations using Vitro-Skin® as a substrate.
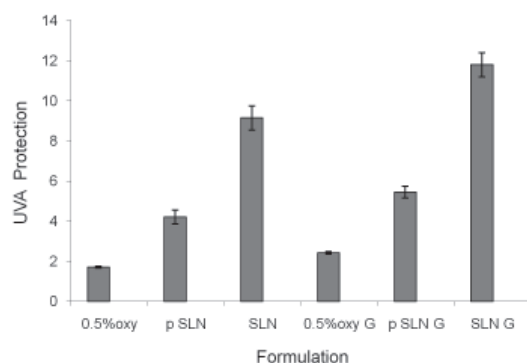
Figure 6. Erythemal UVA protection factor for different SLNs formulations using Vitro Skin® as a substrate.

a very low UVA protection factor of about 1.7 ± 0.05. Conversely, oxybenzone-loaded SLN2 was found to have a high EUVA-PF (9.15 ± 0.6). Since both dispersions contain the same concentration of oxybenzone, the SLN2 formulation was more effective and offered improved photoprotection. This was due to a combination of the reflecting properties of the solid particles and the absorbing characteristics of the oxybenzone (*62*). Due to this synergistic effect, the concentration of a potentially harmful molecular UV blocker can be decreased while maintaining the desired UV protection without needing an additional physical sunscreen (*7*). Lipid matrices may have also contributed to a better SPF and EUVA-PF since they provided a fixation medium for oxybenzone when the suspensions were spread over the substrates (*29*).

The SPF and EUVA-PF results for the prepared gels indicated better protection against UV radiation than that provided by corresponding dispersions. The viscosity values should confirm this observation since increased SPF values always coincide with higher viscosities (*29*).

Sunscreen formulations with a pseudoplastic flow produce a coherent protective film covering the skin surface with an evenly distributed UV filter, and this activity is important for a higher SPF. Newtonian materials do not behave in this way because they run very quickly when spread on the skin, reducing the

protective film. A pseudoplastic material, however, can break down to allow easy spreading, and the applied film can instantaneously gain viscosity to resist running (*19*).

4. Conclusion

The present work has shown that SLNs containing the lipophilic sunscreen oxybenzone can be produced by the solvent diffusion method. The advantage of this method is the instantaneous and reproducible formation of SLNs with a high loading capacity. Oxybenzone is insoluble in water and cannot be readily incorporated in a gel base. Once oxybenzone was entrapped in SLNs, it could be easily incorporated into a gel base without the crystallization problems that are common to oxybenzone. Topical application of a gel formulation containing SLNs of oxybenzone was found to be more efficient at protecting against UVA and UVB radiation. This is probably due to the film formation over the skin, which itself acts as a physical barrier to UV radiation. In conclusion, the results of this study emphasize the potential for SLNs to serve as a new topical drug delivery system. As such, they can enhance the sunscreen efficacy of oxybenzone by about 6-fold while using the minimum required concentration of oxybenzone (0.5%). Encapsulation in SLNs also offers the advantage of overcoming solubility and skin irritancy problems.

References

1. Svobodova A, Walterova D, Vostalova J. Ultraviolet light induced alteration to the skin. Biomed Pap Med Fac Univ Palacky Olomouc Czech Repub. 2006; 150:25-38.
2. Srinivas CR. Photoprotection. Indian J Dermatol Venereol Leprol. 2007; 73:73-79.
3. Wissing S, Müller R. The development of an improved carrier system for sunscreen formulations based on crystalline lipid nanoparticles. Int J Pharm. 2002; 242:373-375.
4. Wissing SA, Müller RH. A novel sunscreen system based on tocopherol acetate incorporated into solid lipid nanoparticles. Int J Cosmet Sci. 2001; 23:233-243.
5. Patel M, Jain SK, Yadav AK, Gogna D, Agrawal GP. Preparation and characterization of oxybenzone-loaded gelatin microspheres for enhancement of sunscreening efficacy. Drug Deliv. 2006; 13:323-330.
6. Benson HA, Sarveiya V, Risk S, Roberts MS. Influence of anatomical site and topical formulation on skin penetration of sunscreens. Ther Clin Risk Manag. 2005; 1:209-218.
7. Wissing SA, Müller RH. Solid lipid nanoparticles (SLN) – a novel carrier for UV blockers. Pharmazie. 2001; 56:783-786.
8. Zhang J, Fan Y, Smith E. Experimental design for the optimization of lipid nanoparticles. J Pharm Sci. 2009; 98:1813-1819.
9. Villalobos-Hernández JR, Müller-Goymann CC. *In vitro* erythemal UV-A protection factors of inorganic

sunscreens distributed in aqueous media using carnauba wax-decyl oleate nanoparticles. Eur J Pharm Biopharm. 2007; 65:122-125.

10. Jermann R, Toumiat M, Imfeld D. Development of an *in vitro* efficacy test for self-tanning formulations. Int J Cosm Sci. 2002; 24:35-42.

11. Springsteen A, Yurek R, Frazier M, Carr KF. *In vitro* measurement of sun protection factor of sunscreens by diffuse transmittance. Anal Chim Acta. 1999; 380:155-164.

12. Hu FQ, Hong Y, Yuan H. Preparation and characterization of solid lipid nanoparticles containing peptide. Int J Pharm. 2004; 273:29-35.

13. zur Mühlen A, Schwarz C, Mehnert W. Solid lipid nanoparticles (SLN) for controlled drug delivery – drug release and release mechanism. Eur J Pharm Biopharm. 1998; 45:149-155.

14. Hu FQ, Jiang SP, Du YZ, Yuan H, Ye YQ, Zeng S. Preparation and characteristics of monostearin nanostructured lipid carriers. Int J Pharm. 2006; 314:83-89.

15. Paliwal R, Rai S, Vaidya B, Khatri K, Goyal AK, Mishra N, Mehta A, Vyas SP. Effect of lipid core material on characteristics of solid lipid nanoparticles designed for oral lymphatic delivery. Nanomedicine. 2009; 5:184-191.

16. Souto EB, Anselmi C, Centini M, Muller RH. Preparation and characterization of *n*-dodecyl-ferulate-loaded solid lipid nanoparticles (SLN®). Int J Pharm. 2005; 295:261-268.

17. Wissing SA, Müller RH. Solid lipid nanoparticles as carrier for sunscreens: *In vitro* release and *in vivo* skin penetration. J Control Release. 2002; 81:225-233.

18. Shah KA, Date AA, Joshi MD, Patravale VB. Solid lipid nanoparticles (SLN) of tretinoin: Potential in topical delivery. Int J Pharm. 2007; 345:163-171.

19. Gaspar LR, Maia Campos PM. Rheological behavior and the SPF of sunscreens. Int J Pharm. 2003; 250: 35-44.

20. Declaration of Helsinki – Current (2008) version. Available at *http://www.wma.net/e/policy/pdf/17c.pdf*

21. Guidelines for Good Clinical Practice. European Medecines Agency. CPMP/ICH/135/95 July 2002

22. Cambell RL, Bruce RD. Comparative dermatotoxicology. I. Direct comparison of rabbit and human primary skin irritation responses to isopropylmyristate. Toxicol Appl Pharmacol. 1981; 59:555-563.

23. Vitro Skin®. 2009. *http://www.ims-usa.com*

24. Diffey BL, Robson J. A new substrate to measure sunscreen protection factors throughout the ultraviolet spectrum. J Soc Cosmet Chem. 1989; 40:127-133.

25. Séhédic D, Hardy-Boismartel A, Couteau C, Coiffard LJ. Are cosmetic products which include an SPF appropriate for daily use? Arch Dermatol Res. 2009; 301:603-608.

26. Mehnert W, Mäder K. Solid lipid nanoparticles: Production, characterization and applications. Adv Drug Deliv Rev. 2001; 47:165-196.

27. Hou D, Xie C, Huang K, Zhu C. The production and characteristics of solid lipid nanoparticles (SLNs). Biomaterials. 2003; 24:1781-1785.

28. Liu J, Gong T, Wang C, Zhong Z, Zhang Z. Solid lipid nanoparticles loaded with insulin by sodium cholate-phosphatidylcholine-based mixed micelles: Preparation and characterization. Int J Pharm. 2007; 340:153-162.

29. Villalobos-Hernández JR, Müller-Goymann CC. Novel nanoparticulate carrier system based on carnauba wax and decyl oleate for the dispersion of inorganic

sunscreens in aqueous media. Eur J Pharm Biopharm. 2005; 60:113-122.

30. Souto EB, Müller RH, Gohla S. A novel approach based on lipid nanoparticles (SLN) for topical delivery of α-lipoic acid. J Microencapsul. 2005; 22:581-589.

31. Rowe RC, Sheskey PJ, Owen SC. Handbook of Pharmaceutical Excipients. 5th ed., Butler & Tanner, Somerset, UK, 2006; pp. 308-310.

32. Siekmann B, Westesen K. Submicron sized parentral carrier systems based on solid lipids. Pharm Pharmacol Lett. 1992; 1:123 -126.

33. Varshosaz J, Minayian M, Moazen E. Enhancement of oral bioavailability of pentoxifylline by Solid lipid nanoparticles. J Liposome Res. 2010; 20:115-123.

34. Schubert MA, Müller-Goymann CC. Solvent injection as a new approach for manufacturing lipid nanoparticles – evaluation of the method and process parameters. Eur J Pharm Biopharm. 2003; 55:125-131.

35. Abdelwahed W, Degobert G, Fessi H. A pilot study of freeze drying of poly(epsilon-caprolactone) nanocapsules stabilized by poly(vinyl alcohol): Formulation and process optimization. Int J Pharm. 2006; 309:178-188.

36. Song X, Zhao Y, Hou S, Xu F, Zhao R, He J, Cai Z, Li Y, Chen Q. Dual agents loaded PLGA nanoparticles: Systematic study of particle size and drug entrapment efficiency. Eur J Pharm Biopharm. 2008; 69:445-453.

37. Guerrero DQ, Fessi H, Allmann E, Doelker E. Influence of stabilizing agents and preparative variables on the formation of poly(D,L-lactic acid) nanoparticles by an emulsification-diffusion technique. Int J Pharm. 1996; 143:133-141.

38. Tiyaboonchai W, Tungpradit W, Plianbangchang P. Formulation and characterization of curcuminoids loaded solid lipid nanoparticles. Int J Pharm. 2007; 337:299-306.

39. Umney N, Rivers S. Conservation of Furniture. Elsevier, Oxford, UK, 2003; pp. 124-193.

40. Mainardes RM, Evangelista RC. PLGA nanoparticles containing praziquantel: Effect of formulation variables on size distribution. Int J Pharm. 2005; 290:137-144.

41. Zimmermann E, Müller RH. Electrolyte- and pH-stabilities of aqueous solid lipid nanoparticle (SLN™) dispersions in artificial gastrointestinal media. Eur J Pharm Biopharm. 2001; 52:203-210.

42. Huang ZR, Hua SC, Yang YL, Fang JY. Development and evaluation of lipid nanoparticles for camptothecin delivery: A comparison of solid lipid nanoparticles, nanostructured lipid carriers, and lipid emulsion. Acta Pharmacol Sin. 2008; 29:1094-1102.

43. Wang Y, Deng Y, Mao S, Jin S, Wang J, Bi D. Characterization and body distribution of β-elemene solid lipid nanoparticles (SLN). Drug Dev Ind Pharm. 2005; 31:769-778.

44. Kumar VV, Chandrasekar D, Ramakrishna S, Kishan V, Rao YM, Diwan PV. Development and evaluation of nitrendipine loaded solid lipid nanoparticles: Influence of wax and glyceride lipids on plasma pharmacokinetics. Int J Pharm. 2007; 335:167-175.

45. Silverman RB. The Organic Chemistry of Drug Design and Drug Action. Elsevier, New York, NY, USA, 2004; pp. 55-61.

46. Yuan H, Miao J, Du YZ, You J, Hu FQ, Zeng S. Cellular uptake of solid lipid nanoparticles and cytotoxicity of encapsulated paclitaxel in A549 cancer cells. Int J Pharm. 2008; 348:137-145.

47. Biehn GF, Ernsberger ML. Polyvinyl alcohol as an emulsifying agent. Ind Eng Chem. 1948; 40:1449-1453.
48. Rebbin V, Jakubowski M, Pötz S, Fröba M. Synthesis and characterisation of spherical periodic mesoporous organosilicas (sph-PMOs) with variable pore diameters. Microporous Mesoporous Mater. 2004; 72:99-104.
49. Wissing SA, Kayser O, Müller RH. Solid lipid nanoparticles for parenteral drug delivery. Adv Drug Deliv Rev. 2004; 56:1257-1272.
50. Souto EB, Wissing SA, Barbosa CM, Müller RH. Development of a controlled release formulation based on SLN and NLC for topical clotrimazole delivery. Int J Pharm. 2004; 278:71-77.
51. Luo Y, Chen D, Ren L, Zhao X, Qin J. Solid lipid nanoparticles for enhancing vinpocetine's oral bioavailability. J Control Rel. 2006; 114:53-59.
52. Yuan H, Huang LF, Du YZ, Ying XY, You J, Hu FQ, Zeng S. Solid lipid nanoparticles prepared by solvent diffusion method in a nanoreactor system. Colloids Surf B Biointerfaces. 2008; 61:132-137.
53. Souto EB, Wissing SA, Barbosa CM, Müller RH. Evaluation of the physical stability of SLN and NLC before and after incorporation into hydrogel formulations. Eur J Pharm Biopharm. 2004; 58:83-90.
54. Doktorovova S, Souto EB. Nanostructured lipid carrier-based hydrogel formulations for drug delivery: A comprehensive review. Expert Opin Drug Deliv. 2009; 6:165-176.
55. Bhaskar K, Mohan CK, Lingam M, Mohan SJ, Venkateswarlu V, Rao YM. Development of Solid lipid nanoparticles and NLC enriched hydrogels for transdermal delivery of nitrendipine: *In vitro* and *in vivo* characteristics. Drug Dev Ind Pharm. 2009; 35:98-113.
56. Liu W, Hu M, Liu W, Xue C, Xu H, Yang X. Investigation of the carbopol gel of solid lipid nanoparticles for the transdermal iontophoretic delivery of triamcinolone acetonide acetate. Int J Pharm. 2008; 364:135-141.
57. Lippacher A, Müller RH, Mäder K. Liquid and semisolid SLN™ dispersions for topical application: Rheological characterization. Eur J Pharm Biopharm. 2004; 58:561-567.
58. Castro GA, Coelho AL, Oliveira CA, Mahecha GA, Oréfice RL, Ferreira LA. Formation of ion pairing as an alternative to improve encapsulation and stability and to reduce skin irritation of retinoic acid loaded in solid lipid nanoparticles. Int J Pharm. 2009; 381:77-83.
59. Küchler S, Wolf NB, Heilmann S, Weindl G, Helfmann J, Yahya MM, Stein C, Schäfer-Korting M. 3D-wound healing model: Influence of morphine and solid lipid nanoparticles. J Biotechnol. 2010; 148:24-30.
60. Wissing SA, Müller RH. Cosmetic applications for solid lipid nanoparticles (SLN). Int J Pharm. 2003; 254:65-68.
61. Song C, Liu S. A new healthy sunscreen system for human: Solid lipid nannoparticles as carrier for 3,4,5-trimethoxybenzoylchitin and the improvement by adding Vitamin E. Int J Bio Macromol. 2005; 36:116-119.
62. Gulbake A, Jain A, Khare P, Jain SK. Solid lipid nanoparticles bearing oxybenzone: *In-vitro* and *in-vivo* evaluation. J Microencapsul. 2010; 27:226-233.